

THE CONTRACTILE PROCESS IN THE CILIATE, *STENTOR COERULEUS*

I. The Role of Microtubules and Filaments

B. HUANG and D. R. PITELKA

From the Department of Zoology and the Cancer Research Laboratory, University of California, Berkeley, California 94720. Dr. Huang's present address is The Rockefeller University, New York 10021.

ABSTRACT

The structural basis for the function of microtubules and filaments in cell body contractility in the ciliate *Stentor coeruleus* was investigated. Cells in the extended state were obtained for ultrastructural analysis by treatment before fixation with a solution containing 10 mM EGTA, 50–80 mM Tris, 3 mM MgSO₄, 7.5 mM NH₄Cl, 10 mM phosphate buffer (pH 7.1). The response of *Stentor* to changes in the divalent cation concentrations in this solution suggests that Ca⁺² and Mg⁺² are physiologically important in the regulation of ciliate contractility. The generation of motive force for changes in cell length in *Stentor* resides in two distinct longitudinal cortical fiber systems, the km fibers and myonemes. Cyclic changes in cell length are associated with (a) the relative sliding of parallel, overlapping microtubule ribbons in the km fibers, and (b) a distinct alteration in the structure of the contractile filaments constituting the myonemes. The microtubule and filament systems are distinguished functionally as antagonistic contractile elements. The development of motive force for cell extension is accomplished by active microtubule-to-microtubule sliding generated by specific intertubule bridges. Evidence is presented which suggests that active shortening of contractile filaments, reflected in a reversible structural transformation of dense 4-nm filaments to tubular 10–12-nm filaments, provides the basis for rapid cell contraction.

INTRODUCTION

The generation of oriented movements in eukaryotic nonmuscle cells has been associated with two basic classes of fibrous elements, microtubules and filaments. Microtubules have been implicated as the structures responsible for chromosomal movement (31, 37), ciliary and flagellar beating (9, 48), and axoplasmic transport (7). At the same time, filamentous structures have been associated with such cellular processes as cytokinesis (50, 52), protoplasmic streaming (44, 63), and morphogenetic cell movements (5, 10, 61). Although it is well documented that both microtubules and

filaments play a role in cell motility, the structural basis and mechanism(s) by which motive force is generated by these fibrous elements remain an area of intensive investigation.

To shed light on the structural basis for the motile functions of microtubules and filaments we have undertaken an analysis of the contractile process in the heterotrichous ciliate, *Stentor coeruleus*. *Stentor* is characterized by extreme changes in cell body length, associated with rapid cell contraction and extreme cell extension. The contractile capabilities of this protozoan are comparable to

those displayed by highly differentiated muscle cells; *Stentor* can contract to 20–25% of its extended length in milliseconds (33, 64).

Stentor's striking contractility has been attributed to two prominent longitudinal fiber systems found in the cell cortex. These two fiber systems, termed by Randall and Jackson (46) the km fibers and myonemes (or M fibers), are characteristic of all contractile heterotrichous ciliates and differ in their fibrous composition (for a review, see reference 42). The km fibers consist of parallel, overlapping ribbons of microtubules, while the myonemes are represented by dense bundles of filaments.

Both cortical fiber systems in *Stentor* are organized parallel to the longitudinal axis of the cell and undergo dimensional changes accompanying changes in cell length. A detailed light microscope analysis of the behavior of the fibers during the contractile process has been presented by Bannister and Tatchell (6). During cell contraction both km fibers and myonemes remain straight, becoming shorter and thicker with decrease in cell length. The behavior of the fiber systems differs during the extension process. At the onset of cell elongation the myonemes are thrown into lateral folds and only with increase in cell length do they straighten. The km fibers, in contrast, remain straight during the entire course of cell elongation, becoming longer and thinner with increase in cell length.

Previous attempts to determine the structural basis for the contractile behavior of the km fibers and myonemes, as well as their functional differentiation, have been hindered by the problem of preserving cells in the extended state for ultrastructural analysis. One of the characteristics of *Stentor* and related contractile ciliates is to contract rapidly upon fixation.

During the course of this study a method was developed which serves to induce cell extension and inhibit contraction of extended cells when exposed to fixatives. Utilizing this method of preserving *Stentor* in the extended state, we have analyzed the structural changes in the km fibers and myonemes that accompany changes in cell length. This study has shed light on the functional differentiation of the two cortical fiber systems in the contractile process and the mechanisms by which they may generate the motive force for changes in cell length.

In the context of eukaryotic contractile

mechanisms, observations on ciliate contractility provide evidence for two distinct models of contractility, the first based on microtubule-to-microtubule sliding generated by intertubule bridges, and the second based on active shortening of contractile filaments.

A preliminary report of this work was presented at the 10th Annual Meeting of the American Society for Cell Biology (26).

MATERIALS AND METHODS

Stentor Cultures

Stentor coeruleus cultures were grown from stocks kindly supplied by Doctors V. Tartar and W. Balamuth. The cultures were maintained in sterile pond water or modified Peter's solution (11) containing a heterogeneous population of microorganisms fed on powdered milk and wheat grains as recommended by Tartar (53).

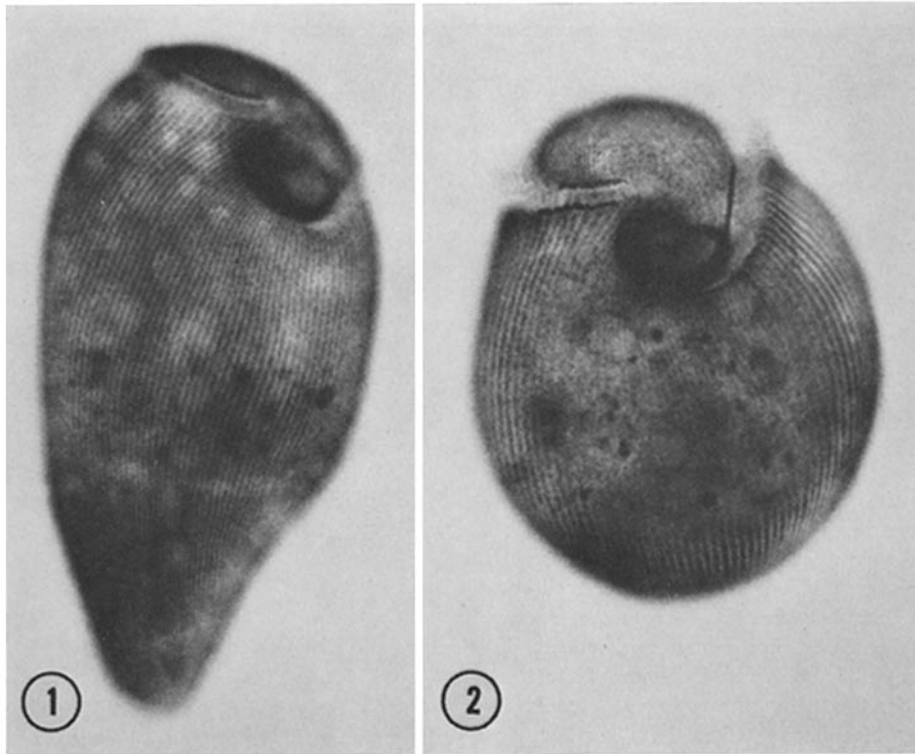
Pretreatment of Cells for

Electron Microscopy

Cells in the extended state were obtained by treatment before fixation with solutions containing 10 mM ethylenebis(oxyethylenenitrilo)tetraacetic acid (EGTA), 50–80 mM Tris, 3 mM MgSO₄, 7.5 mM NH₄Cl, 10 mM phosphate buffer (pH 7.1). Partially extended specimens were obtained by treatment with the above solution in which the MgSO₄ concentration was lowered to 0.5–1.0 mM. After exposing cells to the relaxation solutions for 15–20 min, the fluid was drawn off and fixative added. Contracted cells were mechanically stimulated to contract as fixative was added.

Preparation for Electron Microscopy

During the course of this study, several different fixation procedures were used. The various methods did not produce any detectable differences in the ultrastructure of the contractile fiber systems, although each procedure did preserve certain cellular features better than others. The fixation methods were all based on initial fixation with glutaraldehyde alone or in combination with phosphotungstic acid (PTA) or the nitrogen mustard derivative Tris-(1-aziridiny)-phosphine oxide (TAPO). All fixations were carried out at room temperature and, unless otherwise indicated, the fixatives were buffered with 0.1 M cacodylate (pH 7.3). (a) Glutaraldehyde fixation (G): cells were fixed in 3% buffered glutaraldehyde for 1 h, rinsed briefly in buffer alone, and postfixed in 1% buffered osmium tetroxide for 30 min. (b) Glutaraldehyde-PTA fixation (GP): a



FIGURES 1 and 2 Light micrographs of living *Stentor coeruleus* in the free-swimming (Fig. 1) and contracted (Fig. 2) states. The cell surface bears a series of longitudinal bands consisting of alternate clear and pigmented stripes. $\times 180$.

modification of a fixation procedure reported by Schäfer-Danneel (49). Cells were initially exposed to 12.5% glutaraldehyde + 1% PTA (pH 7.0 adjusted with 1 N KOH) for 1–2 min. The fixation solution was then diluted 1:1 with 4% osmium tetroxide + 1% PTA (pH 7.0 adjusted with 1 N KOH). The cells were fixed in this solution, which has a final concentration of 6.25% glutaraldehyde, 2% osmium, and 1% PTA, for 20–30 min. (c) Glutaraldehyde-TAPO fixation (GT): a modification of a fixation procedure reported by Williams and Luft (62). Cells were initially fixed in 3% buffered glutaraldehyde in the presence of 1% TAPO for 20 min. This was followed by fixation in fresh 3% buffered glutaraldehyde for 2 h. The cells were then rinsed briefly in the buffer and subsequently postfixed in 1% buffered osmium for 30 min.

After fixation, the cells were dehydrated in a graded series of ethanol, passed through propylene oxide, and embedded in Epon 812. Thin sections cut on a Porter-Blum MT-2 were stained with uranyl acetate and lead citrate and examined in a Siemens Elmiskop I at 80 kV.

Descriptive Conventions

The following directional terminology will be used for describing the cortical ultrastructure in *Stentor*. *Anterior* and *posterior* refer to positions on the body of the whole organism. *Right* and *left* denote the two sides of a kinety (longitudinal row of ciliary basal bodies) as viewed by an observer standing inside of the cell looking outward. Electron micrographs of longitudinal sections of the cell cortex are oriented to show components as they would appear to an observer standing inside of the cell looking outward, the anterior end of the cell always toward the top of the picture. Electron micrographs of transverse sections of the cell cortex show components as they would appear to an observer looking from the anterior end of the cell posteriad. Using these conventions, the descriptive directions right and left in all electron micrographs correspond to the reader's handedness. Only in Fig. 12, which is a schematic diagram of the cortex as viewed from outside of the cell, are the right and left sides of a kinety the reverse of the reader's.

RESULTS

EGTA/Mg⁺ Relaxation Solution

Stentor in its free-swimming form approximates a gently rounded cone (Fig. 1), from which the cell can contract to a sphere (Fig. 2) or extend to an elongated trumpet shape (Fig. 3). Rapid contraction is elicited by chemical, electrical, or mechanical disturbances, while elongation to fully extended lengths is generally associated with attachment of cells to a substrate.

Cells in the extended state were obtained by treatment, before fixation, with a solution containing 10 mM EGTA, 50–80 mM Tris, 3 mM MgSO₄, 7.5 mM NH₄Cl, 10 mM phosphate

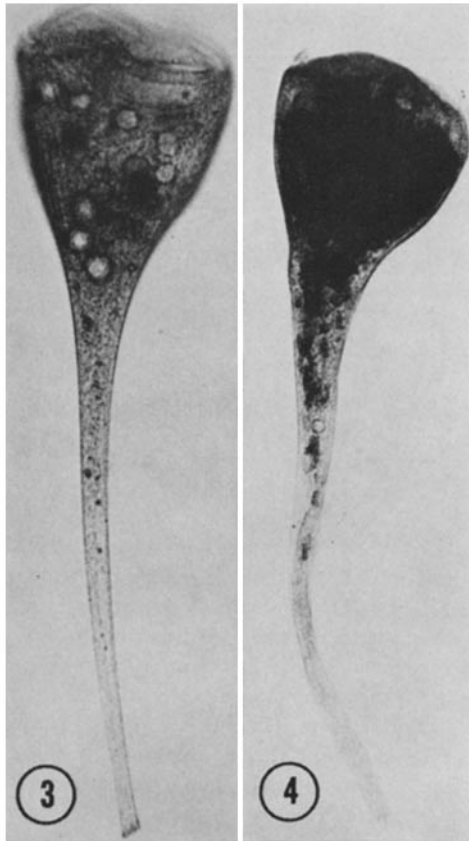


FIGURE 3 Light micrograph of a living cell in the extended state with characteristic elongated-trumpet shape. $\times 90$.

FIGURE 4 Light micrograph of a cell extended in the EGTA/Mg⁺ relaxation solution and subsequently fixed in glutaraldehyde. $\times 90$.

buffer (pH 7.1). Exposure to this relaxation solution induces free-swimming cells gradually to extend to lengths comparable to those observed in nature, 1.0–1.5 mm. Subsequent fixation with glutaraldehyde does not result in any detectable length changes or distortion of the cell shape (compare Fig. 4 with Fig. 3). While cell extension in nature occurs in several seconds, cells in the relaxation solution require 10–15 min to attain maximum extension; otherwise the behavior of the cortical fiber systems during extension in the relaxation solution is identical with that observed by light microscopy in untreated, living cells.

Summarized in Table I are the effects of varying the EGTA and divalent cation concentration on the behavior of the cells and the subsequent results of fixation. The degree of cell elongation occurring in the relaxation solution is dependent on the MgSO₄ concentration. In the absence of MgSO₄ the cells do not undergo any appreciable increase in cell length. The presence of 0.5–1.0 mM MgSO₄ induces cells to extend to approximately two times their contracted lengths. These partially extended cells are generally conical, resembling cells in the free swimming state (see Fig. 1). Raising the MgSO₄ concentration to 2–3 mM results in extension to the elongated trumpet shape.

To prevent contraction of extended cells upon fixation requires the direct inhibition of the generation of motive force for cell contraction. In recent years it has been suggested that calcium plays an important role in the initiation of contraction in ciliates. Glycerinated models of vorticellid ciliate stalks have been shown to be highly sensitive to changes in Ca⁺ levels (2, 25, 35). Recently, Ettienne (12) has demonstrated a direct relationship between intracellular free Ca⁺ levels and the onset of contraction in the ciliate *Spirostomum*. In ciliates microinjected with the calcium-sensitive bioluminescent protein, aequorin, Ettienne recorded an increase in internal Ca⁺ levels associated with the initiation of cell contraction.

The presence of the Ca⁺-chelating agent EGTA in the relaxation solution at a minimum level of around 10 mM effectively prevents extended cells from contracting when exposed to glutaraldehyde (Table I). This inhibitory effect of 10 mM EGTA is counteracted by the addition of 3–5 mM CaCl₂ to the standard relaxation solution. When the CaCl₂ concentration is raised

TABLE I
Effects of Varying EGTA, Mg^{+2} , and Ca^{+2} Concentrations in the Relaxation Solution

	EGTA	$MgSO_4$	$CaCl_2$	Behavior	Effect of fixation
	<i>mM</i>	<i>mM</i>	<i>mM</i>		
Standard solution	10	3	—	Extension	Remain extended
Varying Mg^{+2} conc.	10	—	—	Contract	
	10	0.5–1.0	—	Partial extension	Remain partially extended
	10	2.0–3.0	—	Extension	Remain extended
Varying EGTA conc.	0–5	3	—	Extension	Contract
	6–8	3	—	Extension	Variable
	9–12	3	—	Extension	Remain extended
Varying Ca^{+2} conc.	10	3	1–2	Extension	Variable
	10	3	3–5	Extension	Contract
	10	3	6–10	Cycling	Contract

above 5 mM the cells undergo repeated cycles of slow contraction and extension, eventually contracting when exposed to fixatives. The action of EGTA in inhibiting contraction is presumably at the level of lowering intracellular, rather than simply extracellular, calcium levels. This is evidenced by the fact that the contractile capabilities of *Stentor* are not altered when cells are bathed in calcium-free medium.

The relaxation solution used in this study has been adapted to preserve the contractile heterotrichs *Condylostoma* and *Spirostomum* in the extended states (Huang, unpublished results). The wide-range effectiveness of this solution emphasizes the possible physiological importance of divalent cations in the regulation of ciliate contractile systems.

Organization of the km Fibers and Myonemes

Accounts of the cortical ultrastructure in *Stentor* have been previously published (6, 13, 14, 20, 30, 46). A detailed description of the organization of the km fibers and myonemes is presented here as background for subsequent descriptions of changes in their structure with changes in cell length. New observations on the morphology of the fibers are included in this section.

KM FIBERS: The cell surface of *Stentor coeruleus* bears a series of longitudinal bands consisting of alternate clear and pigmented stripes

(Fig. 5). Single rows of cilia, or kineties, are disposed within the clear zones. The km fibers are longitudinally arrayed immediately below the cell surface in the area of the clear stripes. Between adjacent km fibers, the pigment granules which constitute the pigmented stripes are seen. The km fibers extend the entire length of the cell body and hooklike processes diverge periodically from the fibers toward the row of cilia lying to their left.

In a low magnification electron micrograph of a longitudinal section taken at this level (Fig. 6) the km fibers are found to be composed of parallel, overlapping ribbons of microtubules. Each fiber lies to the right of a row of basal bodies (kinety).

In a higher magnification, longitudinal view of a single km fiber (Fig. 7) the rigid association of the microtubule ribbons and accompanying kinety is seen. Each ribbon is attached at its anterior origin to the posterior, nonciliated basal body of a repeating cortical unit based on a pair of basal bodies. A diagrammatic representation of a single cortical unit is seen in the inset of Fig. 7. The ribbons pass from their origin toward the cell surface, twist to the right, and eventually come to lie in parallel overlapping array with ribbons originating from more anterior and posterior cortical units of the same kinety. In a longitudinal section individual ribbons have been followed for a maximum distance of 15 μ m. Accompanying the microtubule ribbon as it passes to the right are two sets of densely staining fibers. These fibers extend along the edge of the ribbon for a distance of

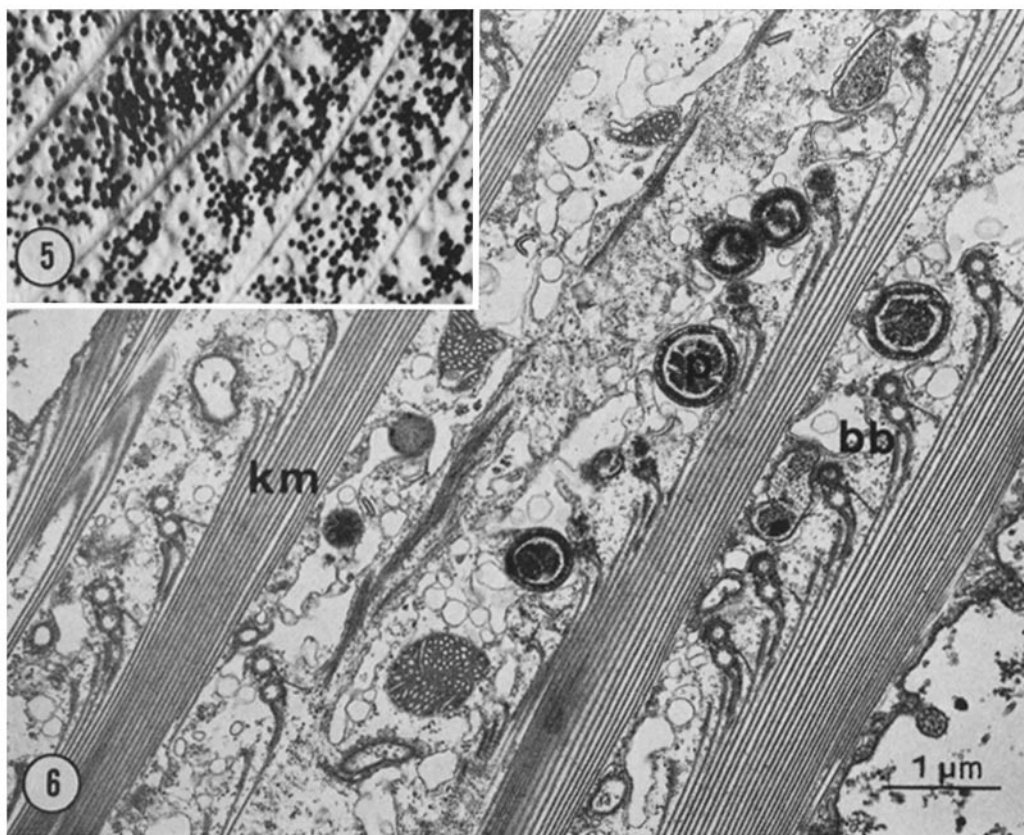


FIGURE 5 Nomarski interference-contrast photomicrograph of the km fibers in a living cell. The fibers extend the entire length of the cell body immediately below the cell surface. Hooklike processes periodically diverge from the fibers toward rows of cilia not visible within the focal plane. Alternating with the km fibers are bands of dense pigment granules. $\times 1,200$.

FIGURE 6 An electron micrograph of a longitudinal section taken at the level of the km fibers (*km*) from a partially extended cell. The fibers consist of parallel, overlapping microtubule ribbons arising in close association with rows of basal bodies (*bb*) lying to their left. Between the fibers, spherical pigment granules (*p*) are seen. Fixation GT. $\times 16,000$.

around $0.7 \mu\text{m}$. Other accessory fiber systems, based on the anterior, ciliated basal body, include an anterior ribbed fiber sheet and a ribbon of left transverse microtubules.

A cross section taken through a single km fiber (Fig. 8) reveals the high degree of organization within individual microtubule ribbons. In most of the ribbons 20 microtubules are arranged in a curved row with a single microtubule lying to the right of the most peripheral microtubule. As prescribed by Bannister and Tatchell (6) the microtubules are numbered 1-21 from the peripheral edge to the internal edge. Toward the side of the km fiber farthest from the accompanying kinety

the number of microtubules per ribbon decreases, with progressive loss of tubules from the internal edge. Since these ribbons represent those transected distal to their origins, it appears that the ribbons are tapered at their ends. Occasionally single microtubules are seen lying free on the right side.

The curvature of the ribbons making up a km fiber is not constant. At the peripheral edge of the km fibers adjacent ribbons are regularly spaced at center-to-center intervals of around 50 nm. Passing internally, the spacing between adjacent ribbons is variable, dependent upon the relative curvature of neighboring ribbons.

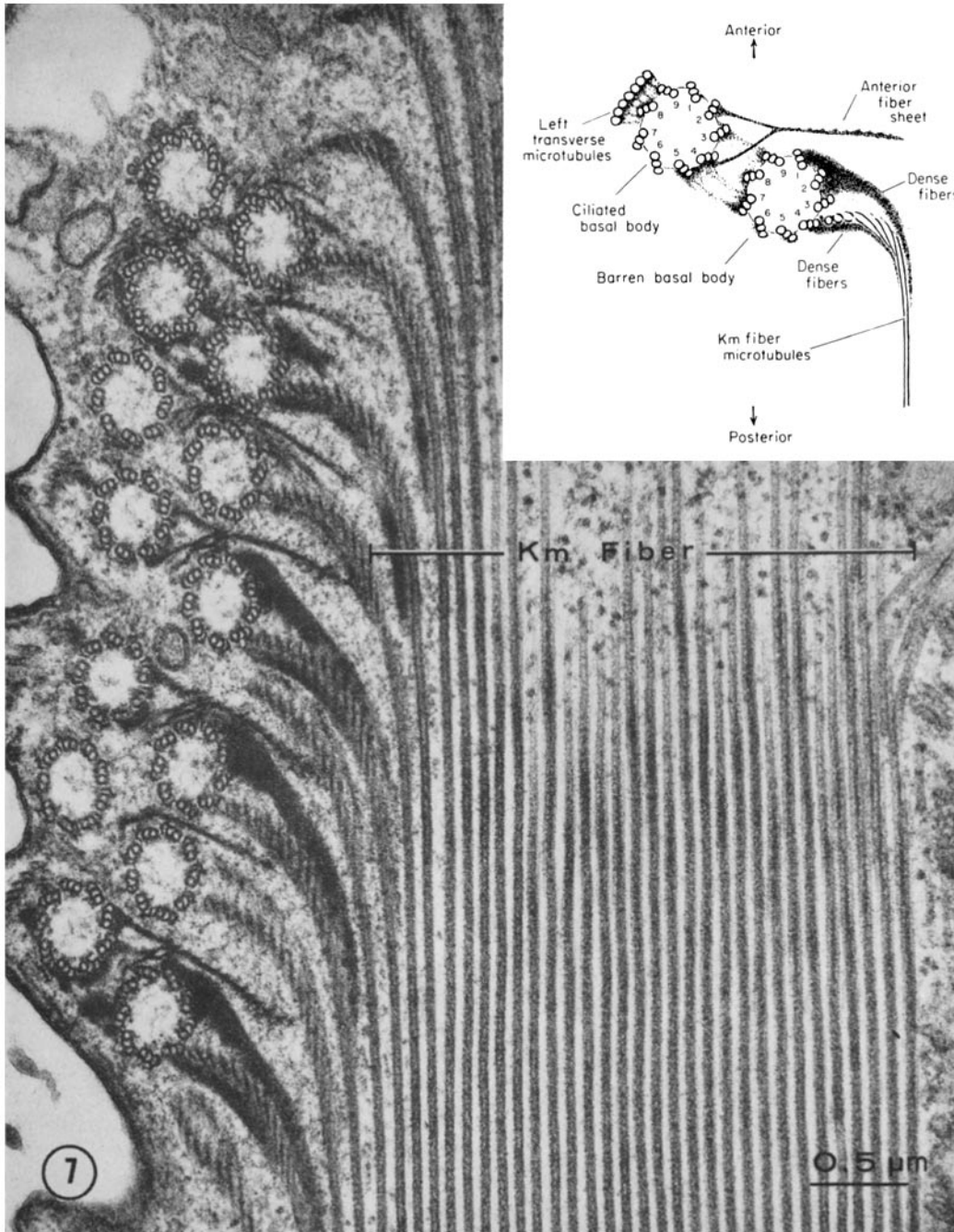


FIGURE 7 An electron micrograph of a longitudinal section of a single km fiber from a contracted cell. The parallel, overlapping organization of the component microtubule ribbons is seen. A repeating cortical unit which lies to the left of the km fiber is schematically diagrammed in the inset. Each microtubule ribbon of the km fiber originates in close association with the no. 4 triplet of the posterior basal body of the cortical unit. The ribbons extend to the right and eventually come to lie in overlapping array with the ribbons originating from the more anterior and posterior cortical units. Accompanying the microtubule ribbons as they pass from their origin are two sets of densely staining fibers. Other accessory fiber systems, which are based on the anterior ciliated basal body, include an anterior ribbed fiber sheet and a ribbon of left transverse microtubules. Fixation GP. $\times 72,000$.

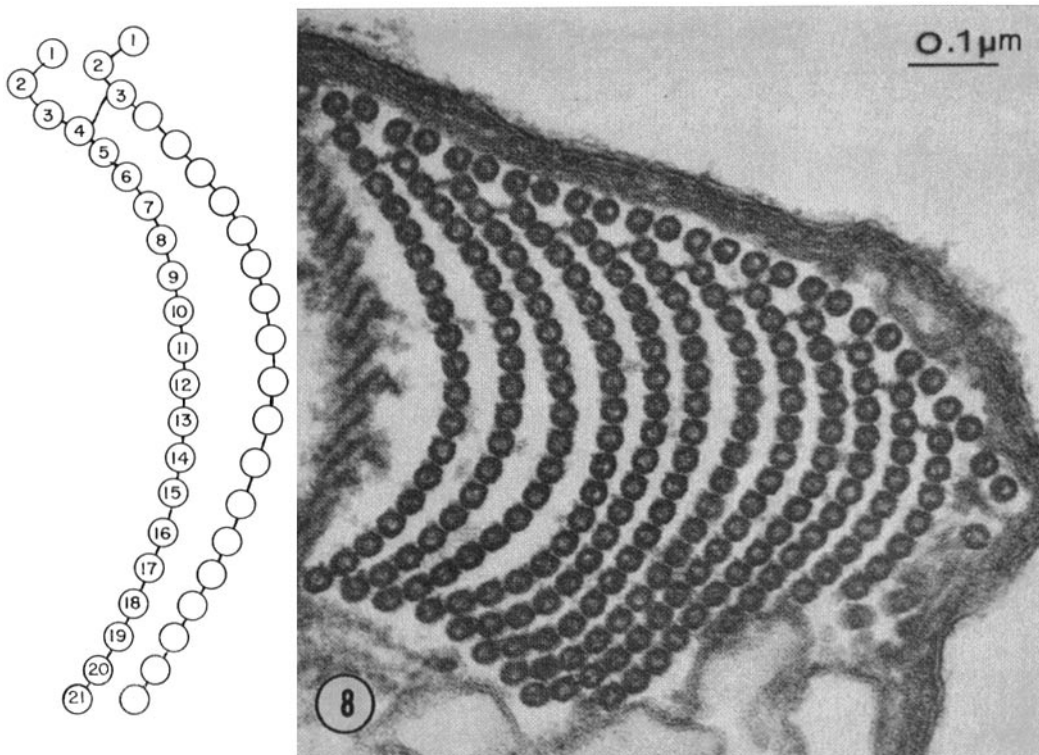


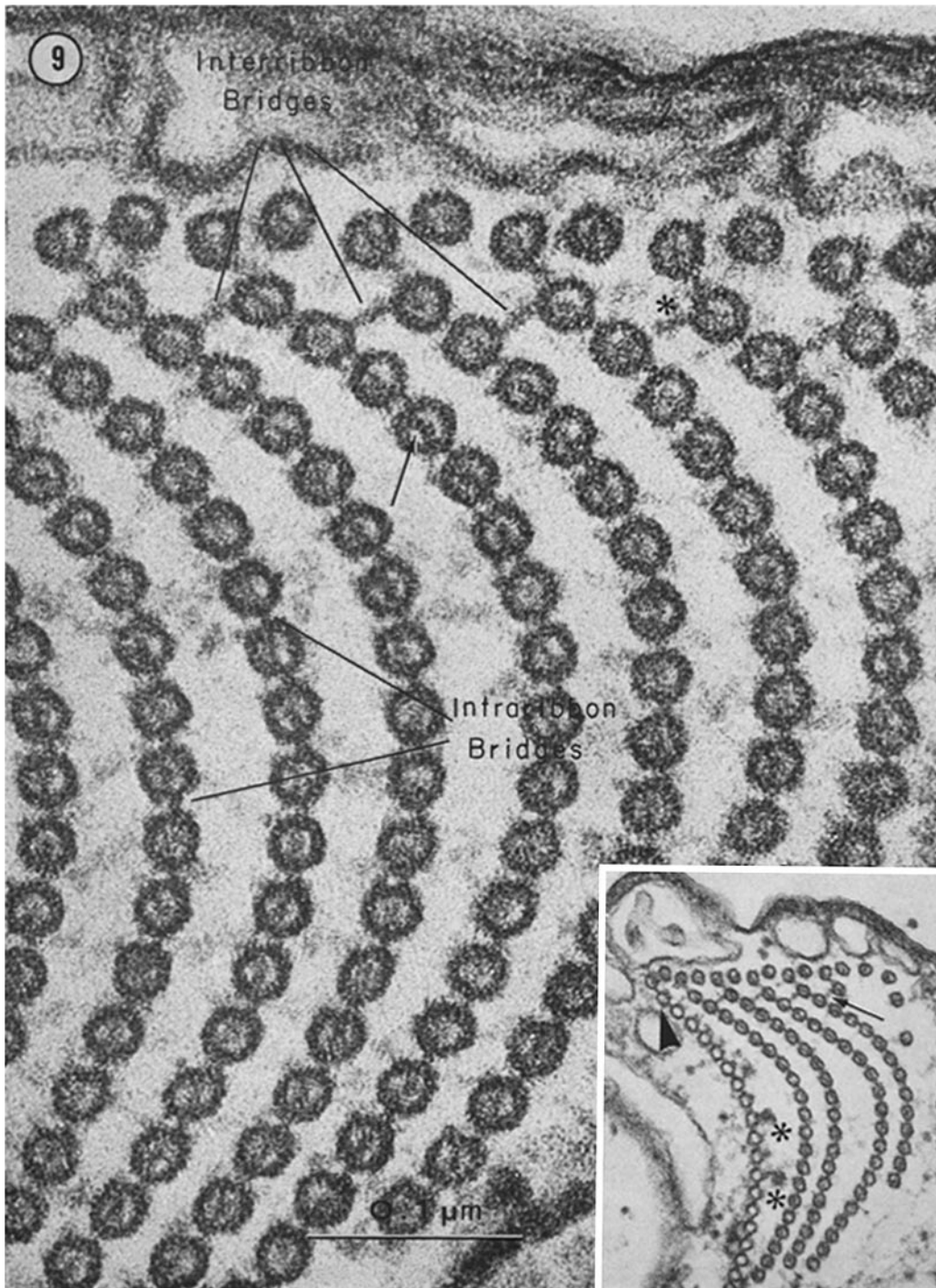
FIGURE 8 An electron micrograph of a transverse section of a single km fiber from an extended cell. Each complete microtubule ribbon consists of 21 tubules arranged in a curved row. As seen on the diagram to the left, the microtubules within a ribbon are numbered consecutively from the peripheral to the internal edge of the ribbons. Fixation G. $\times 120,000$.

The microtubules of the km fibers measure approximately 26–28 nm in diameter, with a wall thickness of 5–6 nm. At higher magnification (Fig. 9) the arrangement of globular subunits within the wall of the microtubules is evident. An unusual feature in the km fibers is the presence of defined substructure within the core of the component microtubules. In most transverse images this internal differentiation is resolved simply as a dense dot in the center of the tubules. Occasionally, however, it appears as a well-defined, 5–6 nm wide, curved septum or bridge across the core of the tubule, always passing in a direction parallel to the curved ribbon axis. The septum does not appear to extend the entire length of the microtubules. In the inset of Fig. 9 we see a km fiber in which the ribbon at the left edge is cut close to its origin, indicated by the presence of associated dense fibrous material. While the microtubules in this ribbon are devoid of internal substructure, microtubules in adjacent ribbons cut more distal

to their origins appear to possess a core differentiation.

The microtubules within each ribbon are linked by cross-bridges, intraribbon bridges (Fig. 9). Between microtubule nos. 3–21 these measure approximately 5 nm in length. The center-to-center spacing of microtubule nos. 1, 2, and 3 is constant, approximately 38 nm, but cross-bridges between these microtubules are not always clearly resolved. When identified, they measure approximately 10 nm in length.

Cross-bridges between adjacent ribbons, interribbon bridges, are a constant feature at the level of the peripheral no. 3 and 4 microtubules. These interribbon bridges, 5–6 nm in width and 18–20 nm in length, always originate from the wall of the no. 3 microtubule of each ribbon and pass to the left toward the no. 4 microtubule on the adjacent ribbon. While the interribbon bridges generally appear straight, they have been observed occasionally to be curved or hooked.



The interribbon bridges do not extend the entire length of the no. 3 microtubules. They arise only after the ribbons come to lie in parallel overlapping array. This is indicated by the fact that interribbon bridges on the no. 3 microtubules are not observed on ribbons transected close to their origin (inset, Fig. 9). On the other hand, the interribbon bridges do appear to extend to the posterior, tapered tip of the ribbons. As seen in the inset of Fig. 9, the interribbon bridge is present on a ribbon represented only by microtubule nos. 1-3.

In transverse images of the km fibers in extended cells (Figs. 8, 9) the interribbon bridges generally appear to be attached at their distal ends to the wall of the no. 4 microtubule on the adjacent ribbon. Examples of detached bridges in extended cells are seen in Fig. 9. Quantitative data on the occurrence of attached vs. detached interribbon bridges in cells fixed at different stages of the contractile process are presented in a subsequent paper.¹

MYONEMES: The myonemes, which consist of dense bundles of filaments, lie immediately below the km fibers (Fig. 10). Unlike the km fibers, the myonemes do not extend the entire length of the cell body; in the anterior third of the cell they taper and lose their fiber organization. The spatial relationship between the two fiber systems is seen in a cross section of the cortex of an extended cell (Fig. 11). The myonemes are surrounded on three

sides by swollen channels of smooth endoplasmic reticulum and occasionally are penetrated by membranous cisternae. The membrane system has often been observed to be continuous with ballooning cisternae of smooth endoplasmic reticulum from the deeper-lying endoplasm. The only structure identified within the cisternae surrounding the myonemes are densely staining bodies ranging from 0.1-0.5 μm in diameter. Groups of mitochondria are frequently localized in the cell cortex. Mitochondria with distensions of the inner and outer membranes are characteristic of cells exposed to the EGTA/ Mg^{+2} relaxation solution. Fig. 12 is a three-dimensional diagram of the cell cortex illustrating the organization and spatial relationship of the contractile fiber systems.

INTERCONNECTIONS: A system of interconnections extending between the microtubule ribbons of the km fiber and the myonemes has been identified (Fig. 13). In a longitudinal section of a km fiber cut parallel to the cell surface (Fig. 13 A), fine 4-nm filaments pass from the right edge of the microtubule ribbons toward the deeper-lying myonemes. These filaments are present only along the anterior length of each ribbon for a distance of around 0.7 μm . In a more oblique section (Fig. 13 B) the interconnections are seen to ramify as they pass internally into a more diffuse network. A longitudinal section perpendicular to the cell surface (Fig. 13 C) reveals how the connecting filaments pass from the microtubule ribbons to interdigitate randomly with the contractile filaments of the myonemes; no specialized attachments have been observed.

¹ Huang, B. The contractile process in the ciliate, *Stentor coeruleus*. II. Axial displacement of microtubules and the role of intertubule bridges. In preparation.

FIGURE 9 A high magnification electron micrograph of the km fiber microtubule ribbons cut in cross section. The microtubules within a ribbon are linked by intraribbon bridges. Passing between adjacent ribbons are distinct interribbon bridges. In extended cells (as seen in this micrograph) the interribbon bridges generally appear attached at both ends. On occasion, a bridge which appears to be detached at its distal end can be seen (*). The central core of the microtubules contains dense substructure. In appropriate images this internal differentiation is resolved as a curved septum extending across the core of the tubule (arrow). Fixation GP. $\times 300,000$. *Inset:* a transverse section of a single km fiber from an extended cell. The microtubule ribbon lying farthest to the left is cut close to its origin, as indicated by the presence of dense fibers (*) lying along its edge. The microtubules within this ribbon are devoid of internal structure. In addition, no interribbon bridge extends from the no. 3 microtubule on this ribbon (arrowhead). The microtubule ribbon lying farthest to the right is cut close to its distal end. In this region, in which the ribbon is represented by only three microtubules, a distinct interribbon bridge is seen to extend from the no. 3 tubule. Fixation GP. $\times 80,000$.

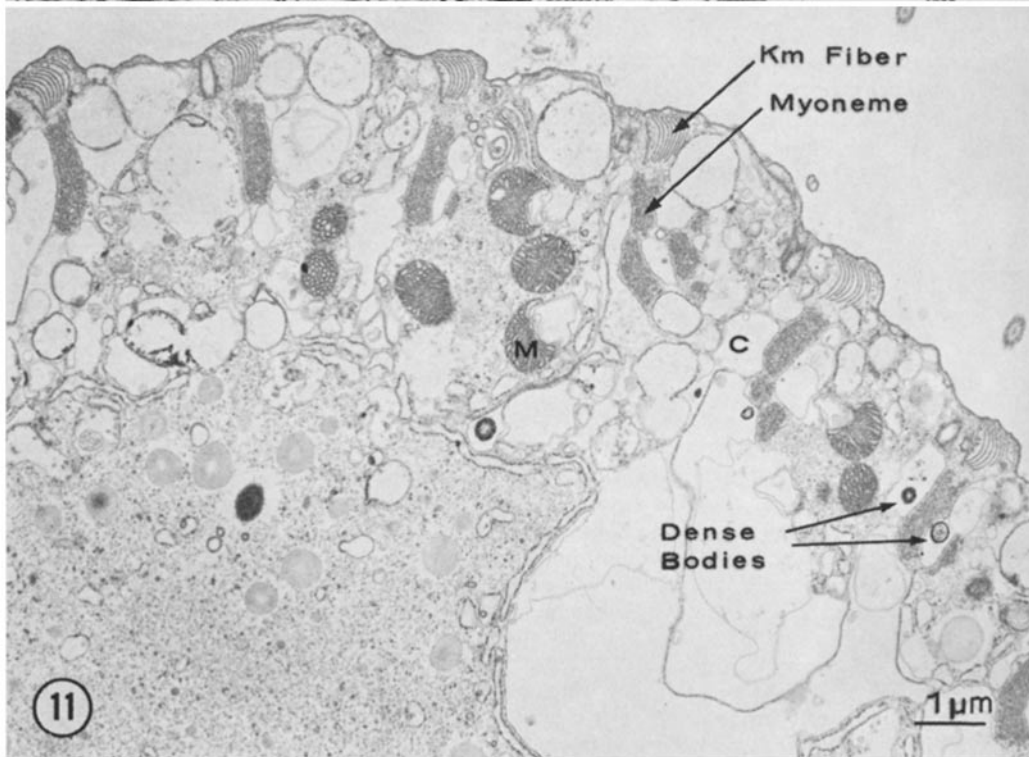
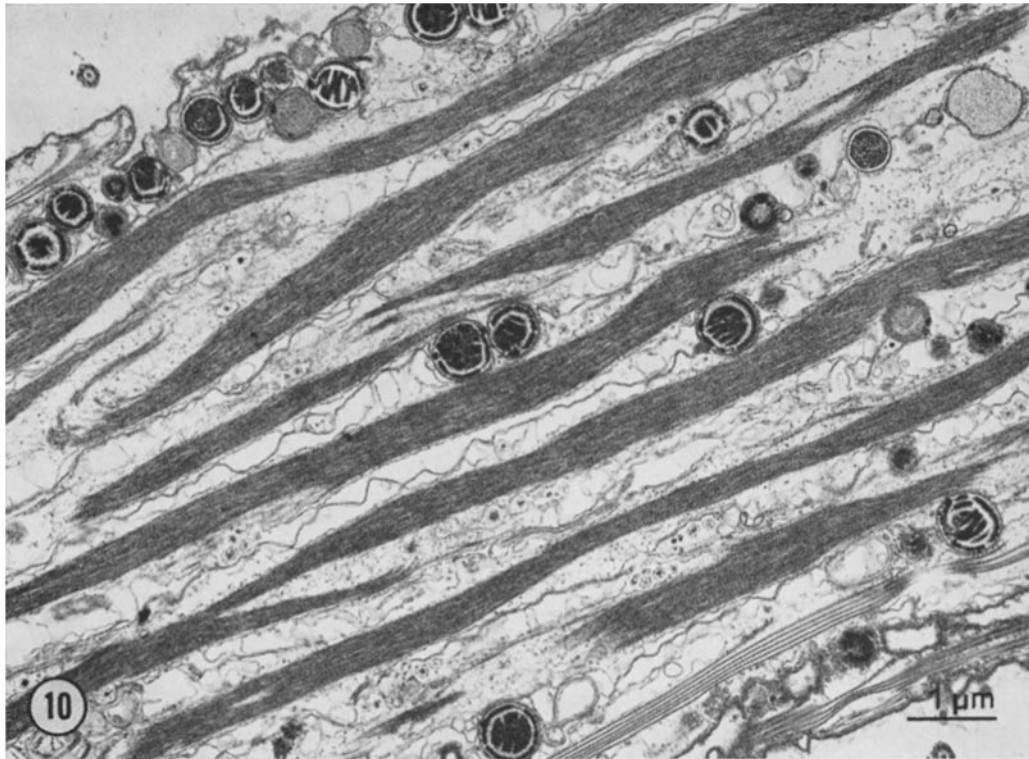


FIGURE 10 An electron micrograph of a longitudinal section of the myonemes from the stalk region of an extended cell. The narrow fibers consist of dense bundles of filaments. Fixation GT. $\times 12,500$.

FIGURE 11 An electron micrograph of a transverse section of the cortex from an extended cell. The myonemes lie immediately below the more superficial km fibers. Ballooning cisternae (C) of smooth endoplasmic reticulum surround the myonemes on three sides. The only structures identified within these distended channels are densely staining bodies. Mitochondria (M) are localized in the cell cortex. Fixation GP. $\times 9,000$.

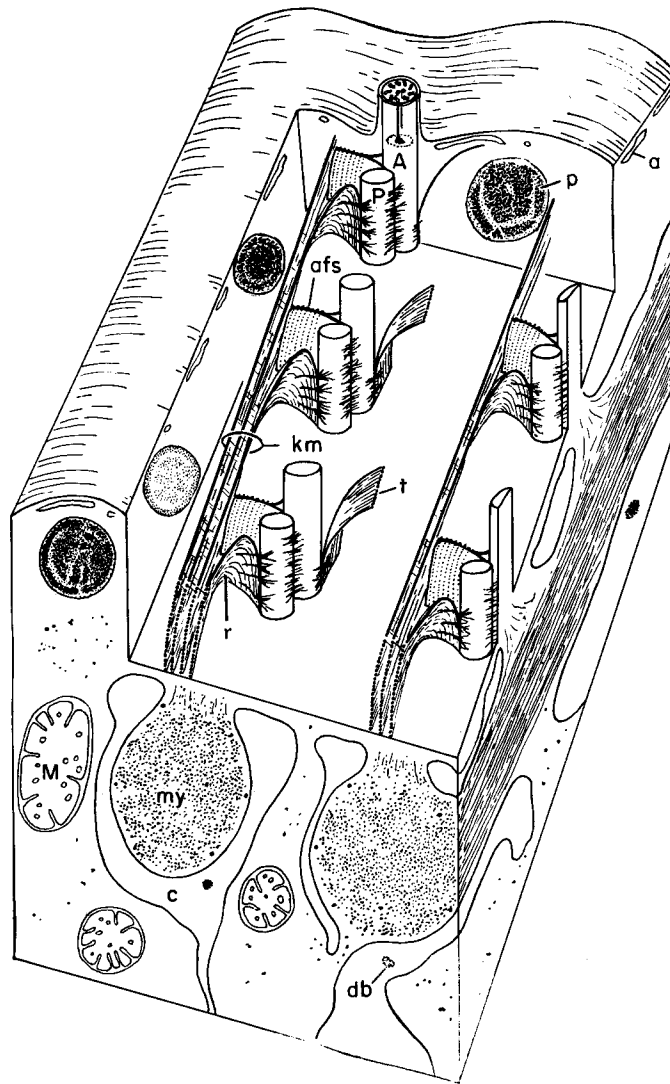


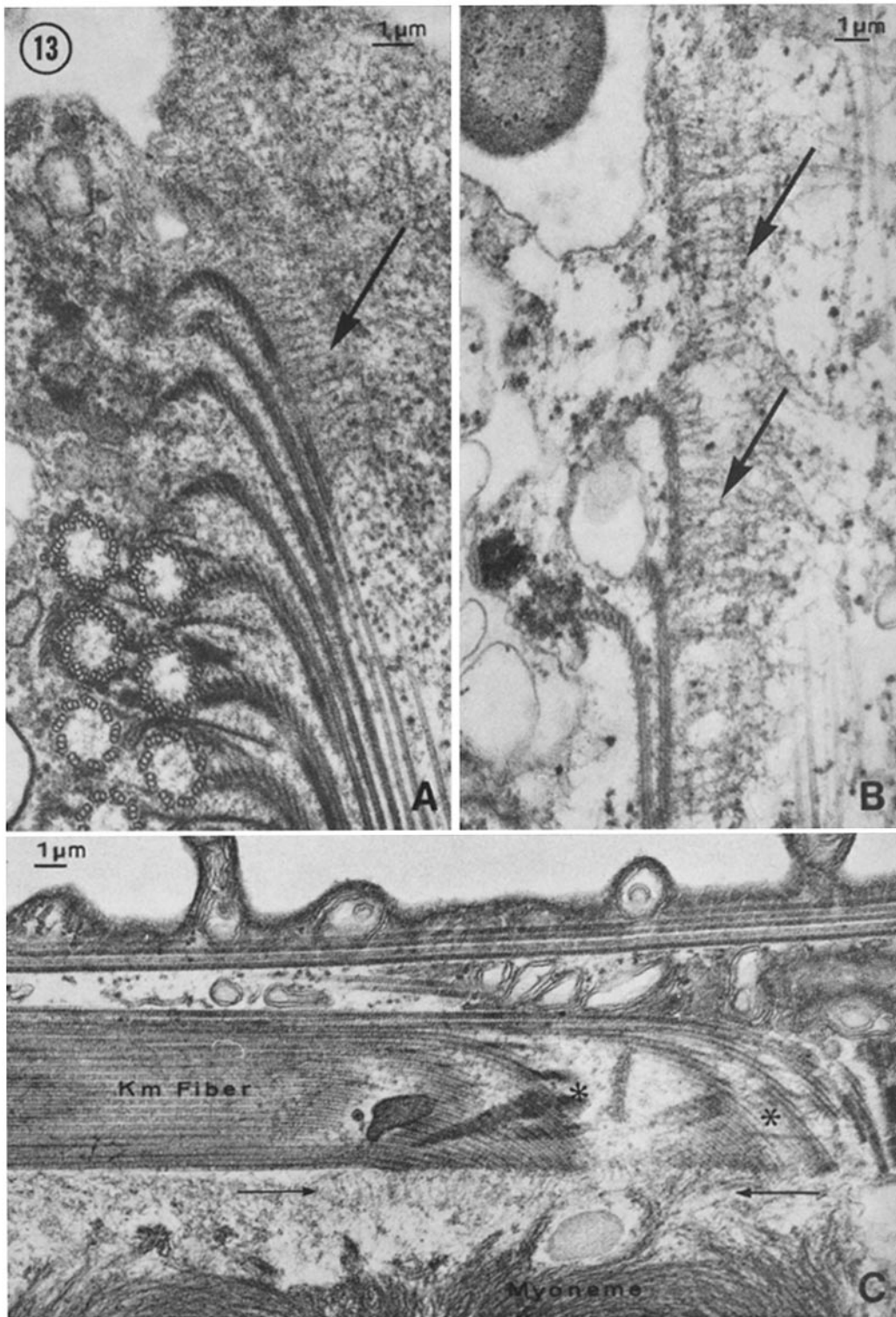
FIGURE 12 A three-dimensional drawing of the somatic cortex in *Stentor coeruleus* illustrating the spatial relationships of the cortical fiber systems. The anterior end of the cell is toward the top of the drawing; the right side of a given kinety is toward the observer's left as viewed from the outside. The various components are labeled as follows: *a*, pellicular alveolus; *p*, pigment granule; *A*, anterior ciliated basal body; *P*, posterior barren basal body; *km*, km fiber; *r*, microtubule ribbon; *afs*, anterior fiber sheet; *t*, transverse microtubules; *my*, myoneme; *M*, mitochondrion; *c*, cisternae of smooth endoplasmic reticulum; *db*, dense body.

Structural Basis for the Contractile Activity of the km Fibers and Myonemes

The organization and structure of the component microtubule ribbons in the km fibers are not altered with changes in cell length. The basis

for the contractile activity of the microtubule system is a variation in the axial position of the parallel, overlapping ribbons relative to one another.

A longitudinal section of a contracted km fiber and its accompanying kinety is seen in Fig. 14. The adjacent basal body pairs within the kinety



are closely apposed with $0.3\ \mu\text{m}$ center-to-center spacing. The overlap of the microtubule ribbons in the km fiber is so extensive that 40 or more ribbons are included in a given cross section of the fiber. The width of the contracted km fibers varies along the length of the cell, increasing posteriorly. In the extreme posterior region, the fibers reach a maximum width of around $2\ \mu\text{m}$, with a maximum number of 78 overlapping ribbons observed in a given km fiber.

In comparison with contracted cells, the km fibers in extended cells are characterized by a striking decrease in the overlap of the microtubule ribbons and a concomitant increase in the distance between adjacent basal body pairs within a kinety. In a longitudinal section through several km fibers from an extended cell (Fig. 15) the basal body pairs, and therefore the points of origin of adjacent microtubule ribbons, are spaced approximately $3\ \mu\text{m}$ apart. The narrow km fibers consist of only four to six overlapping microtubule ribbons. Along the length of extended cells a minimum of two overlapping ribbons per km fiber has been observed. At the posterior end of the cell, the microtubule ribbons terminate a short distance from the cell membrane.

Changes in cell length are associated with alterations in the structure and organization of the contractile filaments in the myonemes. As previously described by Bannister and Tatchell (6), the contracted myonemes in *Stentor* are densely packed with tubular-appearing filaments. In a high magnification longitudinal section through a contracted myoneme (Fig. 16) the highly aggregated state of filaments measuring 10–12 nm in diameter is seen. While the contracted filaments are generally oriented along the longitudinal axis of the fiber they are not strictly parallel in array. Most frequently, individual or groups of filaments are seen oriented at slight angles to one another. In a given section the contracted filaments can be

followed for only short distances of not more than $0.1\ \mu\text{m}$. Analysis of serial sections suggests that this is an accurate reflection of their maximum lengths. Occasionally, small groups of filaments running parallel to one another can be identified. These filaments always appear to be separated along their length by a narrow clear zone.

In transverse images of contracted myonemes (inset, Fig. 16) the tubular nature of the contracted filaments is clearly resolved. The wall of the filaments measures 4–5 nm in width and often appears to be made up of four to six globular subunits.

In contrast to contracted myonemes, which reach a maximum width of approximately $2\ \mu\text{m}$, the fibers in extended cells measure no more than $0.5\ \mu\text{m}$ in diameter. As seen in Fig. 10, the straight and narrow extended myonemes consist of dense bundles of filaments which are clearly oriented along the longitudinal axis of the fibers. The aggregated state of the extended filaments makes an accurate determination of their size and length difficult even at higher magnifications (Fig. 17). While the extended filaments are well oriented, they are somewhat sinuous along their length. As a consequence, in most transverse sections of the myonemes (inset, Fig. 17) the filaments are cut in a variety of planes, producing a meshwork appearance. The dense extended filaments measure approximately 4 nm in diameter. Larger tubular filaments identified in contracted cells are never seen within extended myonemes.

During the initial stages of cell extension the myonemes are thrown into sinuous folds. This convoluted state of the myonemes is clearly resolved on the light microscope level with Nomarski interference optics (Fig. 18 A). In a longitudinal section passing through a single fold of a myoneme from a partially extended cell (Fig. 18 B), dense bundles of filaments identical with those observed

FIGURE 13 Electron micrographs of longitudinal sections of the cell cortex illustrating the organization of fine filaments that extend between the microtubule ribbons of the km fibers and the deeper-lying myonemes. In a section taken parallel to the cell surface (A), fine filaments (arrow) extend periodically from the right edge of a microtubule ribbon as it passes from its origin. In a more oblique section (B) these filaments ramify into a more diffuse network as they pass internally (arrows). In a section taken parallel to the cell surface (C) the filaments form diffuse connections with the deeper-lying myonemes (arrows). The connecting filaments only extend from the edges of the microtubule ribbons as they curve to take on their longitudinal orientation (*). Fixation GP. A, $\times 64,000$; B, $\times 49,000$; C, $\times 42,000$.

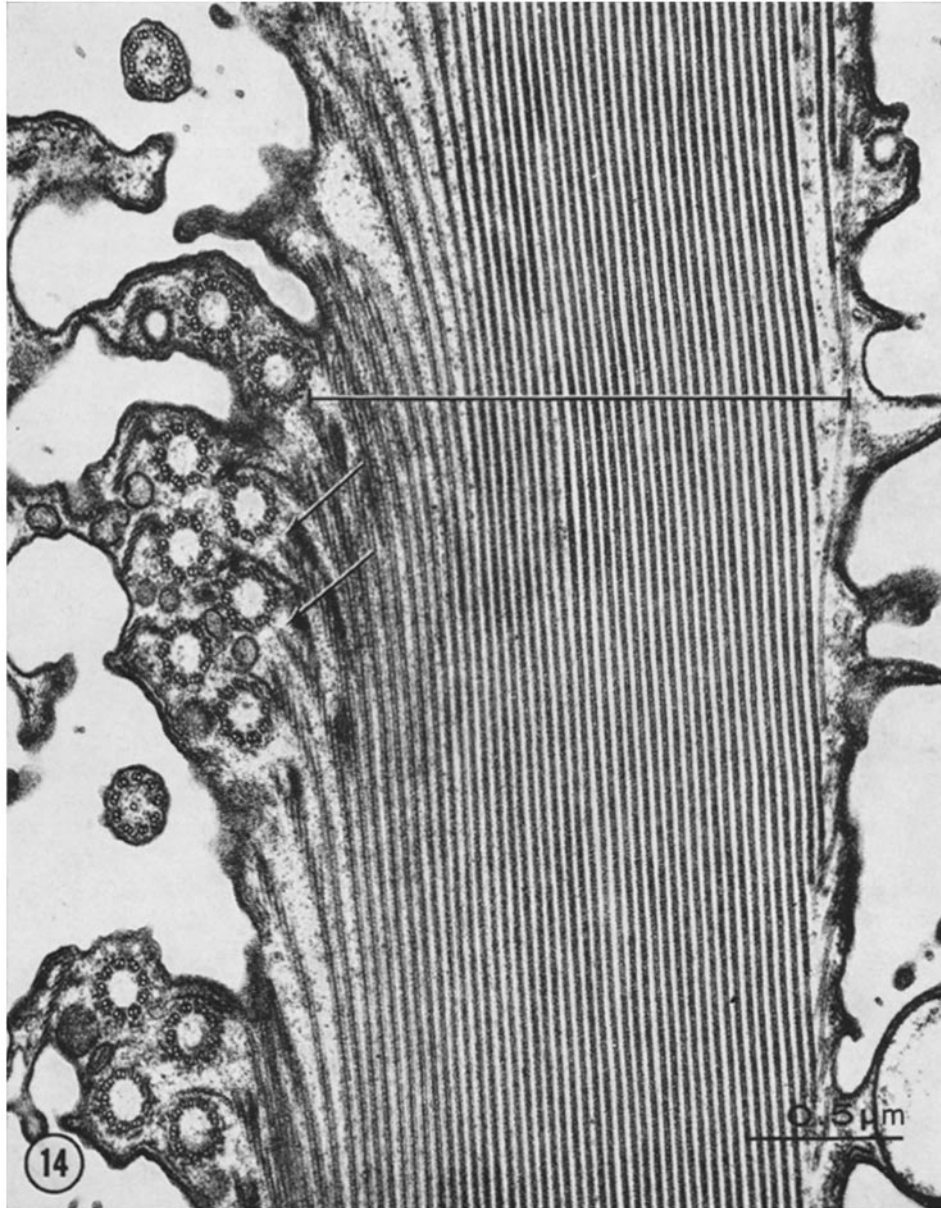


FIGURE 14 An electron micrograph of a longitudinal section through a single contracted km fiber. In a given cross-sectional area of the fiber, 40 or more overlapping microtubule ribbons are seen. The distance between the origins of adjacent ribbons (arrows) is around $0.3 \mu\text{m}$. Fixation GP. $\times 42,000$.

in extended cells are seen. The filaments are oriented along the longitudinal axis of the fiber, closely following its convoluted course. In a transverse section of the cortex from such a cell (Fig. 18 C) the sinuous nature of the 4-nm dense filaments is evident. Larger tubular filaments have not been identified in these cells. In contrast to the

apparent identity in configuration of myoneme filaments in partially extended and extended cells, the morphology of km fibers in partially extended cells resembles that in contracted cells. The km fibers in Fig. 18 C measure around $1.7 \mu\text{m}$ in width and are composed of 25 or more overlapping microtubule ribbons.

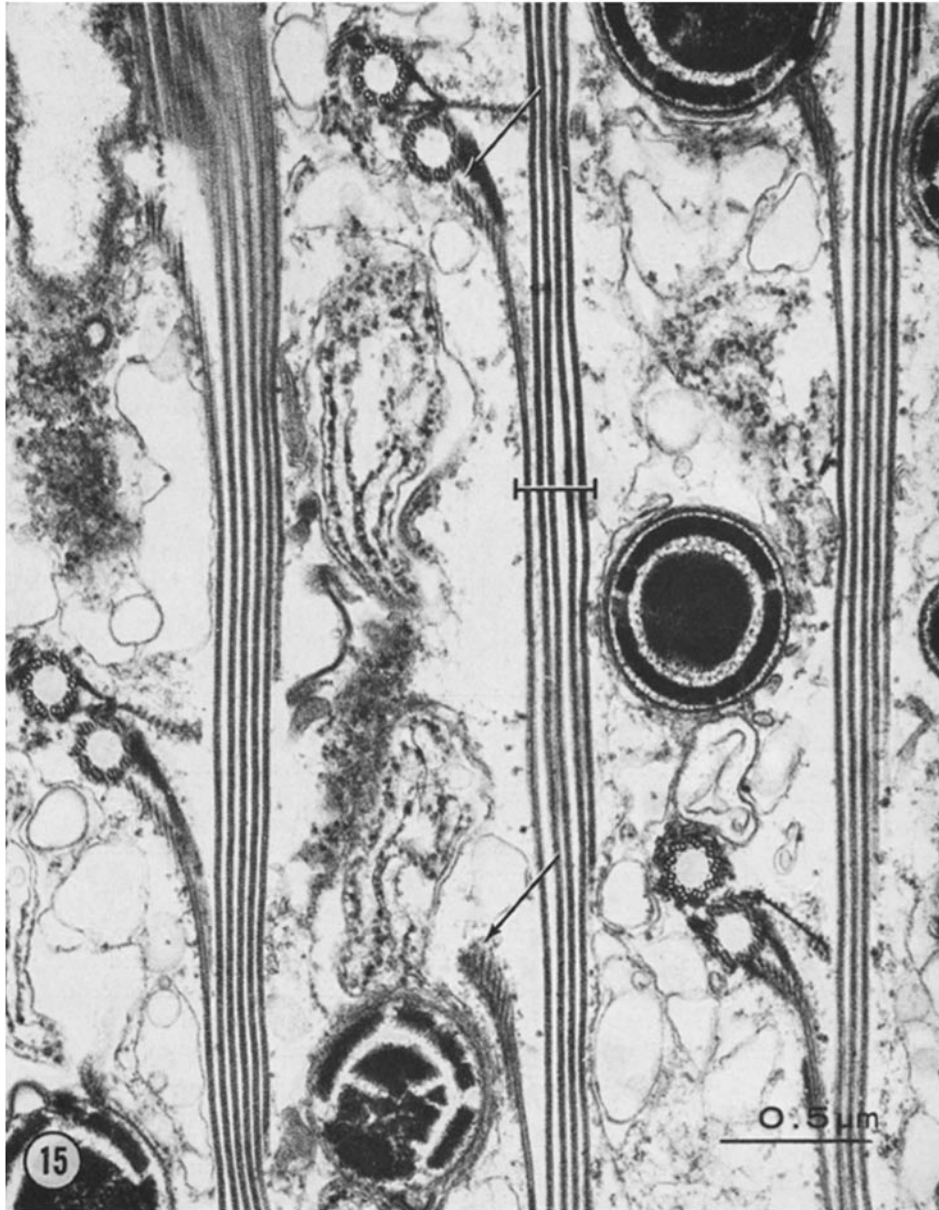


FIGURE 15 An electron micrograph of a longitudinal section through several extended km fibers. In a given cross-sectional area of the fibers, only four to six overlapping microtubule ribbons are seen. The distance between the origins of adjacent ribbons (arrows) is around $3.0 \mu\text{m}$. Fixation GP. $\times 40,000$.

DISCUSSION

Antagonistic Contractile Roles of the km Fibers and Myonemes

Since the first identification of the cortical km fibers and myonemes in *Stentor*, it has been suggested that they serve as the contractile elements

(for reviews, see references 53, 55, 58). However, differentiation of their roles in the contractile process has been difficult. Attempts to selectively disrupt the activity of alternate systems in the living cell have been unsuccessful. Microtubule-disrupting agents, such as colchicine and vinblastine, have been found to have no effect on the

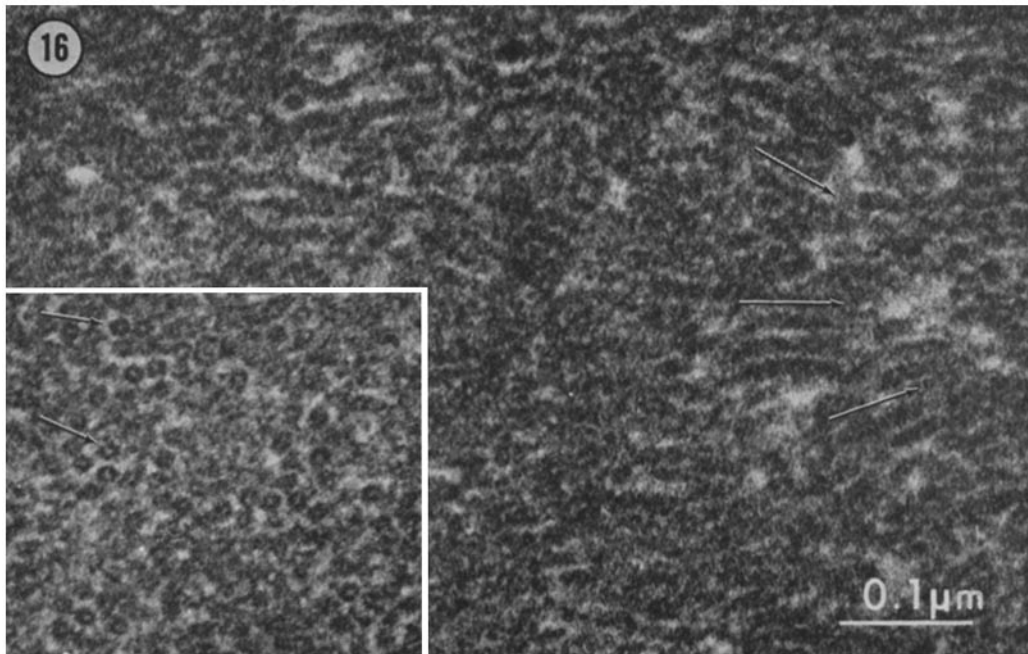


FIGURE 16 An electron micrograph of a longitudinal section through a contracted myoneme. The densely packed filaments are 10–12 nm in diameter. While the filaments are generally oriented along the longitudinal axis of the myoneme fiber, they are not strictly parallel in array. Individual or groups of filaments are oriented at slight angles to one another (arrows). In transverse sections (*inset*) the 10–12-nm filaments appear tubular in profile, with a wall thickness of 4–5 nm. The wall of the filaments sometimes appears to be made up of four to six subunits (arrows). Fixation GP. $\times 180,000$.

contractile behavior of the cell or the preformed structure of the km fiber microtubules (27). At the same time the drug cytochalasin B reported to inhibit movement and to selectively disrupt microfilaments in a variety of cell types (61) does not inhibit contractility in *Stentor* or alter the structure of the myonemes (27).

There are, however, several lines of evidence which suggest that the two fiber systems in *Stentor* may function as antagonistic contractile elements, the filamentous myonemes generating the motive force for cell contraction, and the microtubule km fibers functioning as the active components in cell extension.

Evidence that the myonemes generate the tension for cell shortening comes from a comparative analysis of the ultrastructure of extended, isotonically contracted, and isometrically contracted cells. In the present study the extended and contracted configurations of both the km fibers and myonemes have been described (for a detailed discussion, see subsequent sections). Bannister and

Tatchell (6) have previously described the ultrastructure of *Stentor coeruleus* fixed in the state of isometric contraction. In these cells, which are stimulated to contract while actual change in cell length is mechanically prevented, the morphology of the km fibers resembles what we have described as characteristic of extended cells, i.e., minimum overlap of the parallel microtubule ribbons. In contrast, the substructure of the myonemes in isometrically contracted cells closely corresponds to that observed in contracted cells. Instead of the longitudinally oriented 4-nm dense filaments identified in extended myonemes, tubular 10–12-nm filaments typical of cells fixed in the contracted state are seen. This observation that the development of tension for cell shortening is specifically associated with contraction of the myonemes clearly indicates that the filament system generates the motive force for cell shortening. This conclusion is further supported by recent high speed cinematic analysis of *Stentor* contraction in which it has been observed that shortening of the

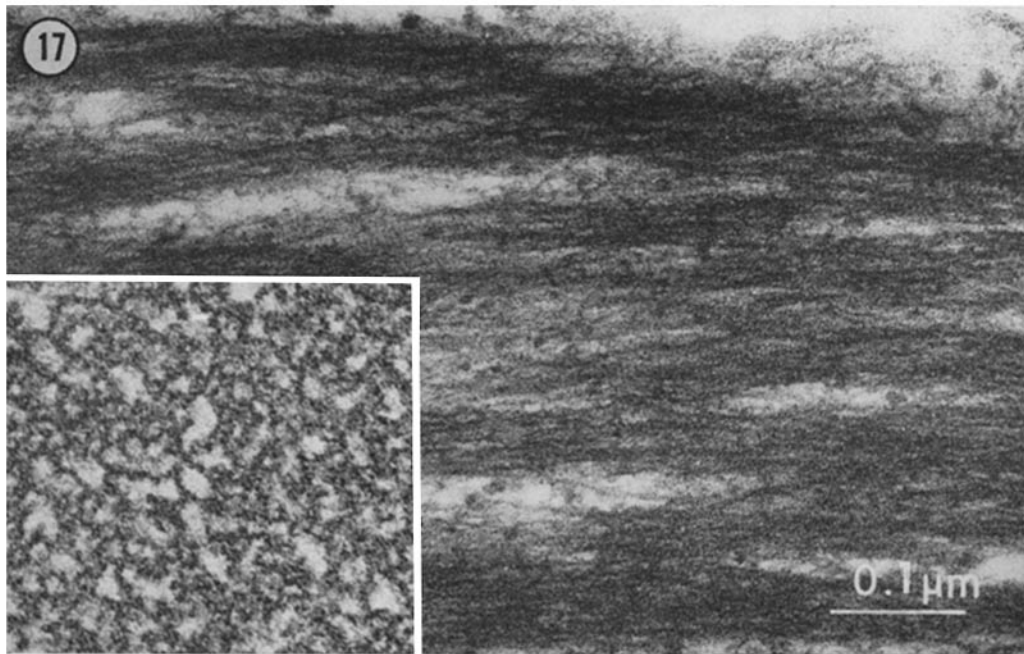


FIGURE 17 An electron micrograph of a longitudinal section through an extended myoneme. The densely aggregated filaments are clearly oriented along the longitudinal axis of the fiber. In transverse sections (*inset*) the somewhat sinuous 4-nm filaments are cut in a variety of planes, producing a meshwork appearance. Fixation GP. $\times 180,000$.

myonemes immediately precedes decrease in cell length (40).

As we have previously noted, *Stentor* displays the ability to vary its extended length from the free-swimming conical form to the elongated trumpet shape. This property of differential extensibility suggests that cell elongation requires an active tension-developing system and is not simply a passive recoil phenomenon. While the myonemes apparently play an active role in cell contraction they do not appear to be actively involved in the extension process. Immediately after a contraction phase and before increase in cell length occurs, the myonemes are observed to undergo folding. In cells fixed in the state of partial extension, the substructure and organization of the filaments in the convoluted myonemes are identical with those observed in extended cells. In contrast, increase in cell length has been found to be strictly correlated with the degree of extension which occurs in the km fibers.¹ These observations, coupled with structural evidence of possible active and passive phases in the activity of the km fibers,¹ support the hypothesis that the generation of motive force for

cell extension resides not in the myonemes but in the microtubule km fibers.

In order for the km fibers and myonemes to function as opposing elements, the forces developed by each fiber system must be transmitted to the alternate system. In the present study the two fiber systems have been observed to be interconnected by fine filaments extending from the anterior region of each microtubule ribbon. Since elongation of the myonemes precedes extension of the km fibers, this spaced series of attachments accounts for the myonemes being forced into lateral folds early in the extension process. With elongation of the km fibers, the distance between the series of myoneme attachments increases, resulting in the gradual unfolding of the myonemes. We suggest that during cell contraction, shortening of the myonemes is translated into the displacement of the km fiber microtubule ribbons via this same system of attachments.

Microtubule-to-Microtubule Sliding

During the contractile process, the organization and structure of the overlapping, parallel micro-

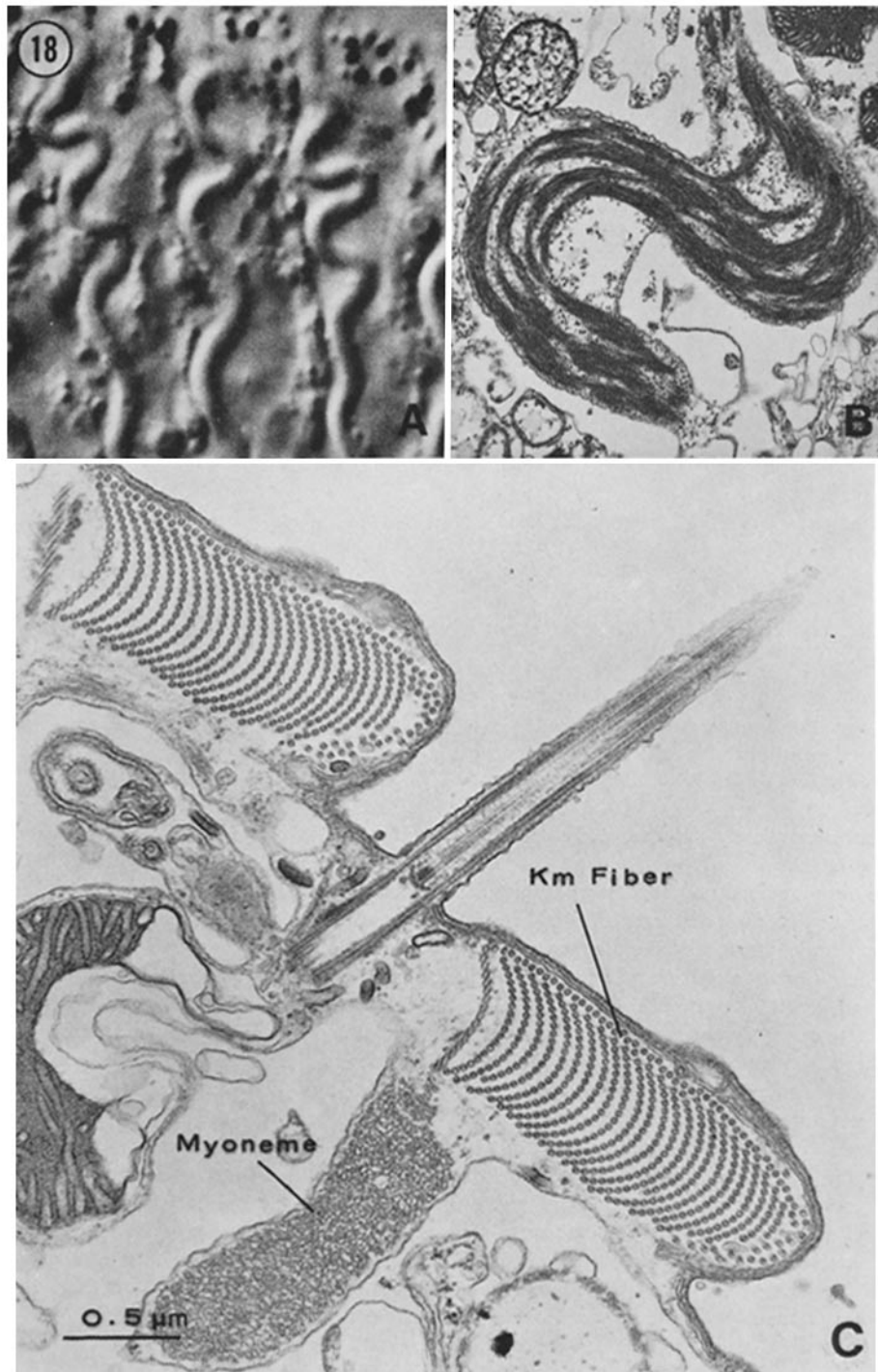


FIGURE 18 (A) A Nomarski interference-contrast photomicrograph of the convoluted myonemes in a living, partially extended cell. $\times 3,000$. (B) An electron micrograph of a longitudinal section through a single myoneme fold of a partially extended cell. Dense bundles of 4-nm filaments are oriented along the longitudinal axis of the fiber, closely following its convoluted course. Fixation GT. $\times 15,000$. (C) An electron micrograph of a transverse section through the cortex of a partially extended cell. Approximately 25 overlapping microtubule ribbons are found within the km fibers. The sinuous nature of the 4-nm dense filaments of the myonemes is seen. Fixation GT. $\times 32,000$.

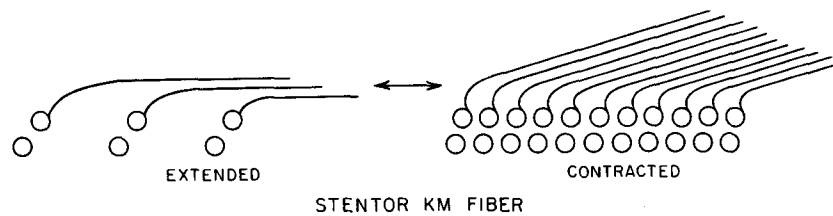


FIGURE 19 A diagram illustrating the relative sliding of the microtubule ribbons in the km fibers that occurs with changes in cell length.

tubule ribbons that make up the km fibers is rigidly maintained. Variations in cell length are correlated with changes in the degree of overlap of adjacent ribbons relative to one another. To accommodate these observed changes, longitudinal displacement or relative sliding of the microtubule ribbons must occur. This sliding-filament model was initially proposed by Randall and Jackson (46) and supported by observations made by Bannister and Tatchell (6) on differences in ribbon overlap in contracted and isometrically contracted cells.

In the km fibers in *Stentor*, each microtubule ribbon slides relative to adjacent ribbons so that concomitant with change in the degree of overlap of the ribbons are (a) change in the distance between origins of adjacent ribbons and (b) change in the number of overlapping ribbons found within a given km fiber cross section (see Fig. 19). It is this latter change that accounts for the dimensional change in the km fibers accompanying changes in cell length.

The parameters for ribbon displacement are governed by the geometry of the system. Since each ribbon is attached at its anterior end to the posterior basal body of a cortical unit, maximum shortening can be defined by the minimum center-to-center spacing between adjacent basal body pairs, around $0.3 \mu\text{m}$. In the posterior region of contracted cells the ribbons approach this maximum degree of overlap, with 78 the largest observed number of overlapping ribbons found in a given km fiber cross section.

The maximum sliding that can take place between adjacent ribbons during the contractile process is defined by the length of the sliding components. In thin sections individual ribbons have been followed for distances of up to $15 \mu\text{m}$. However, multiplying the maximum number of ribbons found in a km fiber cross section (78 ribbons) by the minimum spacing between adjacent basal body pairs ($0.3 \mu\text{m}$) we arrive at a

figure of around $24 \mu\text{m}$ for the maximum length of the ribbons. Data obtained from quantitative analysis of ribbon overlap in *Stentor* fixed in the contracted and extended states¹ suggest that the actual distance that adjacent ribbons are displaced with changes in cell length falls far short of this maximum figure. This study reveals that with a fourfold increase in total cell length, each microtubule ribbon in the km fibers slides relative to adjacent ribbons for an average distance of around $2.0 \mu\text{m}$.

The microtubules of the km fibers fall into the class of stable microtubules (8, 60) in that they resemble those of the ciliary and flagellar axoneme in their response to various antimitotic agents. Exposure of *Stentor* to colchicine or vinblastine sulphate at concentrations of 10^{-6} to 10^{-5} M have no effect on the contractile properties or structure of the km fiber microtubules (27). However, at similar concentrations these agents will inhibit the regeneration of cortical microtubules in *Stentor* and related ciliates (22, 39, 54).

In comparison with axonemal microtubules, those of the km fibers appear to possess a higher degree of linear rigidity. When the microtubule ribbons in *Stentor* are subjected to longitudinal compression, rather than curving or bending, they undergo sharp breaks along their length (27). A septum-like structure has been identified in the electron-lucent core of the km fiber microtubules. The presence of similar internal structure has been previously reported in neurotubules, but assigned no functional significance (41). In the km fibers this core structure is distinctly absent at the anterior region of the fibers where the microtubules curve and then twist upon themselves to take on their parallel, longitudinal orientation. The absence of the internal structure in the region in which the microtubules display linear flexibility and its presence along the rest of their length suggests that it may serve to reinforce the longitudinal rigidity of microtubules, providing the

required framework for a sliding-filament system of active extension.

Fundamental to the sliding-filament model of motility as originally proposed for vertebrate striated muscle is the observation that the overlapping fibrous elements themselves are not contractile, but that motive force is generated by cross-linkages or bridges between the sliding components (for a review, see reference 29).

The occurrence of cross-bridges between microtubules is wide-spread among both protozoan and metazoan cells but their function is still largely unknown. There is evidence that in some instances intertubule bridges are important in the development and maintenance of specific patterns of microtubule arrays (for a review, see reference 56). It has also been proposed that in microtubule-associated systems of motility, intertubule bridges may provide the motive force for relative sliding of parallel arrays of microtubules. Such systems include ciliary motility (47, 48, 51), chromosomal movement (37), nuclear elongation of fowl spermatids (38), and the undulatory motion of the axostyles of oxymonad flagellates (21, 36).

In *Stentor* the 21 microtubules within each ribbon of the km fibers are joined by intraribbon bridges. These bridges serve to cross-link the microtubules into a rigid structural and functional unit. In 1968 Bannister and Tatchell (6) were the first to describe cross-bridges between adjacent microtubule ribbons. These interribbon bridges measure 18–20 nm in length and 5–6 nm in width. They extend from the wall of the no. 3 microtubule and are generally angled toward or attached to the no. 4 microtubule on the adjacent ribbon. The bridges appear in pairs along the length of the no. 3 microtubule with an alternate 9 nm/14 nm center-to-center spacing.¹ These bridges have been observed only along the no. 3 microtubules in the region in which axial displacement of the ribbons can occur. They are distinctly absent along the anterior curved length of the ribbons.

The position of these bridges between the sliding components in the km fibers excludes the possibility that they represent permanent structural cross-linkages. We propose, as has been previously suggested by Bannister and Tatchell (6), that the 3/4 intertubule bridges are active, mechanochemical units capable of functioning in a fashion analogous to muscle cross-bridges to push the ribbons past one another. This hypothesis is supported by evidence that the structure and orientation of the interribbon bridges differ in cells fixed

in various stages of the contractile process.¹ The variation in bridge morphology has been interpreted to suggest that during cell extension the bridges on the no. 3 microtubules react with active sites along the no. 4 microtubules to generate a relative sliding force between adjacent ribbons. The evidence further indicates that, during cell contraction, the bridges are detached to allow for the passive displacement of the ribbons.

While there is no direct evidence that the interribbon bridges in *Stentor* contain enzymes capable of releasing chemical energy from compounds such as ATP, as is found in the cross-bridges in striated muscle (28), there is clear evidence that proteins with enzymatic activity can be associated with microtubules in the form of projections extending from the tubule wall. The best characterized of the microtubule-associated ATPases have been identified in cilia and flagella (18). The major axonemal ATPase, dynein, is found in pairs of arms which project from the wall of each outer fiber toward adjacent fibers (16, 19). Activation of ATPase activity in cilia is dependent on the presence of Mg^{+2} or Mn^{+2} (15, 17). As previously noted, the effectiveness of the relaxation solution used in this study in inducing cell extension requires the presence of Mg^{+2} . By analogy with activation of ciliary motility, in the km fibers in *Stentor* a protein similar to dynein with Mg^{2+} -dependent ATPase activity may be associated with the activation of microtubule sliding during the extension process.

Filament Contraction Model

Recent studies on the functional role of filaments in cell motility have focused attention on the possibility that the mechanism of force generation in "primitive" systems of movement parallels that of differentiated muscle cells (43). This hypothesis has been supported by the identification of actin-like filaments in nonmuscle cells (32), and the isolation of actin- and myosin-like proteins from such diverse sources as sea urchin eggs (24), amoebae (45, 59), intestinal brush border (57), and blood platelets (1).

The question that remains, however, is whether the basis for all motile processes in eukaryotic cells can be defined by the principles of metazoan muscle contraction. Specific physiological properties and morphological changes in the contractile filaments in *Stentor* appear to be inconsistent with a two-component sliding filament mechanism of motility.

The generation of motive force for cell contraction in *Stentor* is correlated with an alteration in the structure of the myoneme filaments. The narrow, extended myoneme fibers consist of longitudinally oriented dense bundles of 4-nm filaments. Although the exact length of the individual extended filaments could not be determined in sectioned material, they appear to be quite long. In contrast, the contracted myonemes are characterized by densely aggregated, tubular-appearing, 10–12-nm filaments of relatively short lengths (less than 0.1 μm). While the chemical identification of the myoneme filaments awaits their isolation and characterization, the dimensional correlation between the 4–5 nm wall thickness of the contracted filaments and the diameter of the extended filaments leads us to propose that the two filament forms may represent different contractile states of a single fibrous element.

The basis for the filament-to-tubule transformation may reside in either linear aggregation or helical coiling of the dense extended filaments. While linear aggregation would account for the subunit organization observed in the wall of the contracted filaments, it would not explain the apparent length differences between the two filament forms. In contrast, a transition involving coiling of individual extended filaments upon themselves would effectively result in their simultaneous shortening and tubularization. In analogy with other fibrous proteins, such as F-actin (23) and the protofilaments of microtubules (4), the 4-nm extended filaments may represent a fibrous polymer of globular subunits. Helical coiling of such filaments would give rise to a subunit appearance in the wall of the resulting tubule.

The proposed filament transformations and the initiation of contraction in *Stentor* are highly dependent upon calcium ion concentrations, but do not appear to require the enzymatic hydrolysis of adenosine triphosphate (ATP). Studies on glycerinated models of *Stentor* reveal that in the absence of added ATP extended cells are activated to contract when the free Ca^{+2} concentration in the bathing solution is raised above a threshold level of 10^{-7} M.² Similar observations have been made on glycerinated models of vorticellid ciliate stalks (2, 25, 35, 60). Stalk models will undergo

² Huang, B., and D. Mazia. The contractile process in the ciliate, *Stentor coeruleus*. III. Active shortening of contractile filaments. In preparation.

repeated cyclic changes in length when the concentration of free Ca^{+2} is altered between 10^{-6} and 10^{-8} M (2). Calcium-activated contraction of such models can be elicited even in the presence of the inhibitors salygran, KCN, dinitrophenol, and 2,4-dinitro-1-fluorobenzene (2, 25).

Observing that ATP-splitting and metabolic activity are not required for activation of contraction in model systems, Hoffman-Berling (25) was the first to suggest that the generation of motive force for ciliate contraction is associated with a configurational change in the contractile filaments brought about by the direct charge interaction of Ca^{+2} with reactive sites along their length. The significance of the charge properties of calcium in the activation of ciliate contraction is evidenced by the observation that contraction in *Stentor*, as well as in vorticellid stalks, can be induced by replacing Ca^{+2} with equal concentrations of Ba^{+2} or Sr^{+2} (25, footnote 2). In the case of Ba^{+2} - and Sr^{+2} -initiated contraction in *Stentor*, a structural change in the contractile filaments identical to that observed with Ca^{+2} -activated contraction is seen.² In contrast with these other divalent cations, Mg^{+2} at concentrations as high as 10^{-2} M will not induce contraction of *Vorticella* or *Stentor* models (2, footnote 2). This suggests some degree of specificity in the activity of Ca^{+2} .

While these studies on the physiology of contraction in *Stentor* and vorticellid ciliates suggest a common mechanism for force generation, changes in the substructure of the contractile filaments similar to those described in *Stentor* have not been observed in related ciliates. In the contractile heterotrichs *Spirostomum* and *Condylostoma* the extended myonemes consist of a network of filaments similar to those observed in *Stentor* fixed in the extended state (34; Huang and Pitelka, unpublished results). Contraction in these cells has been found to be associated with only a slight increase in aggregation of the extended filaments, without the appearance of larger tubular forms. Similar observations have been made on living and glycerinated models of vorticellid ciliate stalks (3; Huang and Hamamoto, unpublished results).

While evidence of active shortening of the contractile filaments in related ciliates has eluded thin section electron microscopy, studies on changes in the birefringence of the contractile fiber (spasmoneme) in vorticellids tend to support such a model (2). In the extended state, the contractile fiber in the living stalks of *Carchesium* is positively birefringent with respect to its length.

With contraction the birefringence falls and the spasmoneme becomes totally isotropic. This loss in birefringence may be a reflection of a change in filament configuration that is not resolved with thin section electron microscopy.

The evidence of dimensional changes in the contractile filaments in *Stentor*, coupled with observations on the physiology of ciliate contraction are interpreted to suggest that in some systems of motility motive force may be generated by the active shortening of a contractile fibrous polymer. Confirmation of this hypothesis awaits further analysis and characterization of these contractile filaments.

We thank Dr. Robert Allen for providing the light micrographs taken with Nomarski interference optics and Mrs. Emily Reid for the diagrams. We are grateful to Doctors D. Mazia and P. Satir for valuable discussions during the course of this study.

This work was supported in part by United States Public Health Service Grants CA-05388 and GM-13882.

The manuscript was prepared while Dr. Huang was a research fellow at the Department of Anatomy, Harvard Medical School, supported by National Institute of Child Health and Human Development 69-2107.

Received for publication 1 August 1972, and in revised form 22 February 1973.

REFERENCES

1. ADELSTEIN, R. S., T. D. POLLARD, and W. M. KUEHL. 1971. Isolation and characterization of myosin and two myosin fragments from blood platelets. *Proc. Natl. Acad. Sci. U. S. A.* **68**:2703.
2. AMOS, W. B. 1971. Reversible mechanochemical cycle in the contraction of *Vorticella*. *Nature (Lond.)* **229**:127.
3. AMOS, W. B. 1972. Structure and coiling of the stalk in the peritrich ciliates, *Vorticella* and *Carchesium*. *J. Cell Sci.* **10**:95.
4. ANDRÉ, J., and J. P. THIÉRY. 1963. Mise en évidence d'une sous-structure fibrillaire dans les filaments axonématiques des flagelles. *J. Microsc. (Paris)* **2**:71.
5. BAKER, P. C., and T. E. SCHROEDER. 1967. Cytoplasmic filaments and morphogenetic movement in the amphibian neural tube. *Dev. Biol.* **15**:432.
6. BANNISTER, L. H., and E. C. TATCHELL. 1968. Contractility and the fibre systems of *Stentor coeruleus*. *J. Cell Sci.* **3**:295.
7. BARONDES, S. H. 1967. Axoplasmic transport. *Neurosci. Res. Program Bull.* **5**:307.
8. BEHNKE, O., and A. FORER. 1967. Evidence for four classes of microtubules in individual cells. *J. Cell Sci.* **2**:169.
9. BROKAW, C. J. 1968. Mechanisms of sperm movement. *Symp. Soc. Exp. Biol.* **22**:101.
10. CLONEY, R. A. 1966. Cytoplasmic filaments and cell movements: Epidermal cells during ascidian metamorphosis. *J. Ultrastruct. Res.* **14**:300.
11. DE TERRA, N. 1966. Culture of *Stentor coeruleus* on *Colpidium campylum*. *J. Protozool.* **13**:491.
12. ETTIENNE, E. M. 1970. Control of contractility of *Spirostomum* by dissociated calcium ions. *J. Gen. Physiol.* **56**:168.
13. FAURÉ-FREMIET, E., and C. ROULLER. 1958. Myonèmes et cinétodesmes chez les ciliés du genre *Stentor*. *Bull. Microsc. Appl.* **8**:117.
14. FAURÉ-FREMIET, E., C. ROULLER, and M. GAUCHERY. 1956. Les structures myoïdes chez les ciliés. Etude au microscope électronique. *Arch. Anat. Microsc. Morphol. Exp.* **45**:139.
15. GIBBONS, B. H., and I. R. GIBBONS. 1969. Reactivation of sea urchin sperm after extraction with Triton X-100. *J. Cell Biol.* **43**(2, Pt. 2): 43 a. (Abstr.)
16. GIBBONS, I. R. 1965. Chemical dissection of cilia. *Arch. Biol.* **76**:317.
17. GIBBONS, I. R. 1966. Studies on the adenosine triphosphatase activity of 14S and 30S dynein from cilia of *Tetrahymena*. *J. Biol. Chem.* **241**:5590.
18. GIBBONS, I. R. 1968. The biochemistry of motility. *Annu. Rev. Biochem.* **37**:521.
19. GIBBONS, I. R., and A. J. ROWE. 1965. Dynein: A protein with adenosine triphosphatase activity from cilia. *Science (Wash. D.C.)* **149**:424.
20. GRAIN, J. 1968. Les systèmes fibrillaires chez *Stentor igneus* Ehrenberg et *Spirostomum ambiguum* Ehrenberg. *Protistologica* **4**:27.
21. GRIMSTONE, A. V., and L. R. CLEVELAND. 1965. The fine structure and function of the contractile axostyles of certain flagellates. *J. Cell Biol.* **24**:387.
22. HAIGHT, J. M., and B. R. BURCHILL. 1970. The effects of colchicine and colcemid on oral differentiation in *Stentor coeruleus*. *J. Protozool.* **17**:139.
23. HANSON, J., and J. LOWY. 1963. The structure of F-actin and of actin filaments isolated from muscle. *Nature (Lond.)* **172**:530.
24. HATANO, S., H. KONDO, and T. MIKI-NOUMURA. 1969. Purification of sea urchin egg actin. *Exp. Cell Res.* **55**:275.

25. HOFFMAN-BERLING, H. 1958. Der Mechanismus eines neuen Kontraktionszyklus. *Biochim. Biophys. Acta.* **27**:247.
26. HUANG, B. 1970. Ultrastructure of the cortical fiber systems in *Stentor coeruleus* relaxed in ethylenebis - (oxyethylenenitrilo) tetraacetic acid. *J. Cell Biol.* **47**(2, Pt. 2):92 a.
27. HUANG, B. 1971. The contractile process in the ciliate *Stentor coeruleus*. Doctoral Thesis. University of California, Berkeley.
28. HUXLEY, H. E. 1963. Electron-microscopic studies on the structure of natural and synthetic protein filaments from muscle. *J. Mol. Biol.* **7**:281.
29. HUXLEY, H. E. 1969. The mechanism of muscular contraction. *Science (Wash. D.C.)*. **164**:1356.
30. INABA, R. 1961. Electron-microscope study on the fine structure of *Stentor coeruleus*. *Bull. Biol. Soc. Hiroshima Univ.* **10**:35.
31. INOUE, S., and H. SATO. 1967. Cell motility by labile association of molecules. *J. Gen. Physiol.* **50**:259.
32. ISHIKAWA, H., R. BISCHOFF, and H. HOLTZER. 1969. Formation of arrowhead complexes with heavy meromyosin in a variety of cell types. *J. Cell Biol.* **43**:312.
33. JONES, A. R., T. L. JAHN, and J. R. FONSECA. 1970. Contraction of protoplasm. III. Cinematographic analysis of the contraction of some heterotrichs. *J. Cell Physiol.* **75**:1.
34. LEHMAN, W. J., and L. J. REBHUN. 1971. The structural elements responsible for contraction in the ciliate *Spirostomum*. *Protoplasma.* **72**:153.
35. LEVINE, L. 1956. Contractility of glycerinated *Vorticella*. *Biol. Bull.* **111**:319.
36. MCINTOSH, J. R. 1971. Microtubule contraction and sliding associated with cellular motility. Abstracts 11th Annual Meeting of the American Society for Cell Biology, New Orleans. 186.
37. MCINTOSH, J. R., P. K. HEPLER, and D. G. VAN WIE. 1969. Model for mitosis. *Nature (Lond.)*. **224**:659.
38. MCINTOSH, J. R., and K. R. PORTER. 1967. Microtubules in the spermatids of a domestic fowl. *J. Cell Biol.* **35**:153.
39. NEVIACKAS, J. A., and L. MARGULIS. 1969. The effect of colchicine on membranellar band regeneration in *Stentor coeruleus*. *J. Protozool.* **16**:165.
40. NEWMAN, E. 1972. Contraction in *Stentor coeruleus*: a cinematic analysis. *Science (Wash. D.C.)*. **177**:447.
41. PETERS, A., and J. E. VAUGHN. 1967. Microtubules and filaments in the axons and the astrocytes of early post-natal rat optic nerves. *J. Cell Biol.* **32**:113.
42. PITELKA, D. R. 1969. Fibrillar systems in protozoa. In *Research in Protozoology*. T. T. Chen, editor. Pergamon Press Inc., New York. **3**:280.
43. POLLARD, T. D. 1972. Progress in understanding amoeboid movement at the molecular level. In *Biology of Amoeba*. K. Joen, editor. Academic Press Inc., New York. 291.
44. POLLARD, T. D., and S. ITO. 1970. Cytoplasmic filaments of *Amoeba proteus*. I. Role of filaments in consistency changes and movement. *J. Cell Biol.* **46**:267.
45. POLLARD, T. D., E. SHELTON, R. WEIHING, and E. D. KORN. 1970. Ultrastructural characterization of F-actin isolated from *Acanthamoeba castellanii* and identification of cytoplasmic filaments as F-actin by reaction with rabbit heavy meromyosin. *J. Mol. Biol.* **50**:91.
46. RANDALL, J. T., and S. F. JACKSON. 1958. Fine structure and function in *Stentor polymorphus*. *J. Biophys. Biochem. Cytol.* **4**:807.
47. SATIR, P. 1965. Studies on cilia. II. Examination of the distal region of the ciliary shaft and the role of the filaments in motility. *J. Cell Biol.* **26**:805.
48. SATIR, P. 1968. Studies on cilia. III. Further studies on the cilium tip and a "sliding filament" model of ciliary motility. *J. Cell Biol.* **39**:77.
49. SCHÄFER-DANNEEL, S. 1967. Strukturelle und Funktionelle Voraussetzungen für die Bewegung von *Amoeba proteus*. *Z. Zellforsch. Mikrosk. Anat.* **78**:441.
50. SCHROEDER, T. E. 1970. The contractile ring. I. Fine structure of dividing mammalian (Hela) cells and the effects of cytochalasin B. *Z. Zellforsch. Mikrosk. Anat.* **109**:431.
51. SUMMERS, K. E., and I. R. GIBBONS. 1971. Adenosine triphosphate-induced sliding of tubules in trypsin-treated flagella of sea-urchin sperm. *Proc. Natl. Acad. Sci. U. S. A.* **68**:3092.
52. SZOLLOSI, D. 1970. Cortical cytoplasmic filaments of cleaving eggs. A structural element corresponding to the contractile ring. *J. Cell Biol.* **44**:192.
53. TARTAR, V. 1961. The biology of *Stentor*. Pergamon Press Ltd., Oxford.
54. TARTAR, V., and D. R. PITELKA. 1969. Reversible effects of antimetabolic agents on cortical morphogenesis in the marine ciliate *Condylostoma magnum*. *J. Exp. Zool.* **172**:201.
55. TAYLOR, C. V. 1941. Fibrillar systems in ciliates. In *Protozoa in Biological Research*. G. N. Calkins and F. M. Summers, editors. Columbia University Press, New York. 191.
56. TILNEY, L. G. 1971. Origin and continuity of microtubules. In *Origin and Continuity of*

- Cell Organelles. J. Reinert and H. Ursprung, editors. Springer-Verlag New York Inc., New York. 222.
57. TILNEY, L. G., and M. MOOSEKER. 1971. Actin in the brush border of epithelial cells of the chicken intestine. *Proc. Natl. Acad. Sci. U. S. A.* **68**:2611.
 58. VILLENEUVE-BRACHON, S. 1940. Recherches sur les ciliés hétéotriches. *Arch. Zool. Exp. Gen.* **82**:1.
 59. WEIHING, R., and E. D. KORN. 1969. Amoeba actin: The presence of 3-methylhistidine. *Biochem. Biophys. Res. Commun.* **35**:906.
 60. WEIS-FOGH, T., and W. B. AMOS. 1972. Evidence for a new mechanism of cell motility. *Nature (Lond.)*. **236**:301.
 61. WESSELLS, N. K., B. S. SPOONER, J. F. ASH, M. O. BRADLEY, M. A. LUDUENA, E. L. TAYLOR, J. T. WRENN, AND K. M. YAMADA. 1971. Microfilaments in cellular and developmental processes. *Science (Wash. D.C.)*. **171**:135.
 62. WILLIAMS, N. E., and J. H. LUFT. 1968. Use of a nitrogen mustard derivative in fixation for electron microscopy and observations on the ultrastructure of *Tetrahymena*. *J. Ultrastruct. Res.* **25**:271.
 63. WOHLFARTH-BOTTERMAN, K. E. 1964. Differentiations of the ground cytoplasm and their significance for the generation of the motive force of amoeboid movement. In *Primitive Motile Systems*. R. D. Allen and N. Kamiya, editors. Academic Press Inc., New York. 79.
 64. WOOD, D. C. 1970. Electrophysiological studies of the protozoan, *Stentor coeruleus*. *J. Neurobiol.* **1**:363.